metals

MDPI

Article

Effect of Crown Shape of Rolls on the Distribution of Stress and Elastic Deformation for Rolling Processes

Rumualdo Servin [1,*], Sixtos A. Arreola [1], Ismael Calderón [1], Alejandro Perez [1] and Sandra M. San Miguel [2]

[1] Facultad de Ingeniería Mecánica y Eléctrica, Barranquilla S/N Col. Guadalupe, Monclova 25280, Mexico; sxtsaav@gmail.com (S.A.A.); ing.ismael.calderon@gmail.com (I.C.); aperezal22@gmail.com (A.P.)

[2] Universidad Tecnológica de la Región Centro de Coahuila, Maintenance and Technology, Carretera 57 Km 14.5, Monclova 25710, Mexico; sandryiza_16@hotmail.com

* Correspondence: rumualdo.servin@uadec.edu.mx; Tel.: +52 1 8666435757

Received: 16 October 2019; Accepted: 10 November 2019; Published: 14 November 2019

Abstract: The present work analyzes the influence of crown shape on the distribution of stresses and deformation for rolling processes. This study consists of a Finite Element Analysis considering combinations of crown shape for Back Up Roll and Work Roll, rolling forces, properties of materials and dimensions of rolls and strip. An analysis of the rolls based on a double cantilever model with the fulcrum of the beams in a centerline mill was carried out. The results show that maximum stress concentrations for all combinations of crown shape analyzed appear on both sides 787.4 mm from the mill centerline, exactly on the sides of the strip. In this area, the maximum stress for the best combination of crown shape is larger than in the centerline mill, increasing from 34.2 MPa to 163.0 MPa. This is proportional according to Hooke's law for which strain of rolls increases from 3.4067×10^{-4} to 4.8368×10^{-4}. The worst combinations of crown shapes were obtained when the shapes of the barrel are the same for the BUR and WR; for example: Combination 1 (BUR Positive–WR Positive), Combination 5 (BUR Flat–WR Flat), and Combination 9 (BUR Negative–WR Negative).

Keywords: back up roll (BUR); work roll (WR); rolling process; stress distribution; finite element analysis (FEA); strain; deformation; distribution of pressure

1. Introduction

One of the most important problems in rolling processes is the control of pressure on the strip. This phenomenon has great influence on the quality of the strip, and the control of this process requires extensive study of each variable, such as wear, crown control, and stress distribution.

Strip flatness and crown control are the basis of strip shape quality. There have been many studies focusing on this issue using mathematical models and the Finite Element Method (FEM). Yang et al. [1] studied the backup roll (BUR) contour in smart crown tandem cold mills. Li et al. [2] conducted the same study for a hot rolling mill. Wang et al. [3] used a negative crown in work rolls (WR). Wang et al. and Cao et al. [4,5] carried out the same study for a hot rolling mill using a Continuous Variable Crown (CVC) in the backup rolls and the work rolls. Liu et al. [6] complemented these studies by considering axial forces in the analysis; and all of them concluded that the contact pressure concentration that exists between work and backup rolls have direct influence on the shape and quality of the strip. The thermal crown is another factor that influences the control of flatness and occurs in cold rolling mills. However, it is more critical in hot rolling mills applications. Chang, Galantucci and Tricarico, Hacquin et al. and Zhao et al. [7–10] concluded that the thermal crown is generated with its maximum point in the center of the rolls, and it is more severe in work rolls due to direct contact with the strip, so an

adequate cooling system must be used to avoid excessive wear. Li et al. [11] states that the Bending Force compensates for the effects of the thermal crown and wear.

The wear on the work rolls is a topic widely studied by S. Spuzic and Strafford, Turk et al. and Li et al. [12–14], and their studies specify that wear increases as the rolling campaign progresses. Rumualdo et al. [15] states that wear becomes more critical in BUR because the rolling campaigns are longer than in the WR. Also, the WRs remain for several hours in each campaign, while the BURs have lamination campaigns of at least fourteen days.

Liu et al. [16] conducted an analysis of rolling pressure along the strip width in cold rolling process, and Zhang et al. [17] did the same analysis for a hot rolling strip; both studies concluded that the peak of maximum pressure concentration was generated at the end of the body in the backup rolls. Kong et al. and Cao et al. [18,19] complemented this study by analyzing different widths of the strip, and as a preventive measure to reduce the concentration of stress, they analyzed different types of chamfers at the ends of the body for the backup rolls.

Liu et al. [6] analyzed the rolls using a double cantilever model with the fulcrum of the beams in a centerline mill for their study of four-high CVC, and Jiang et al. [20] used the same mathematical model in order to theoretically analyze the cold rolling process using an ultra-thin strip with roll edge kiss.

When the stress concentration is not controlled, excessive wear can be generated, which affects the pressure distribution, and in extreme cases, there are operational accidents with cracks and fractures of rolls at the ends of the work barrel as shown in the images of Figure 1a for BUR and Figure 1b for WR.

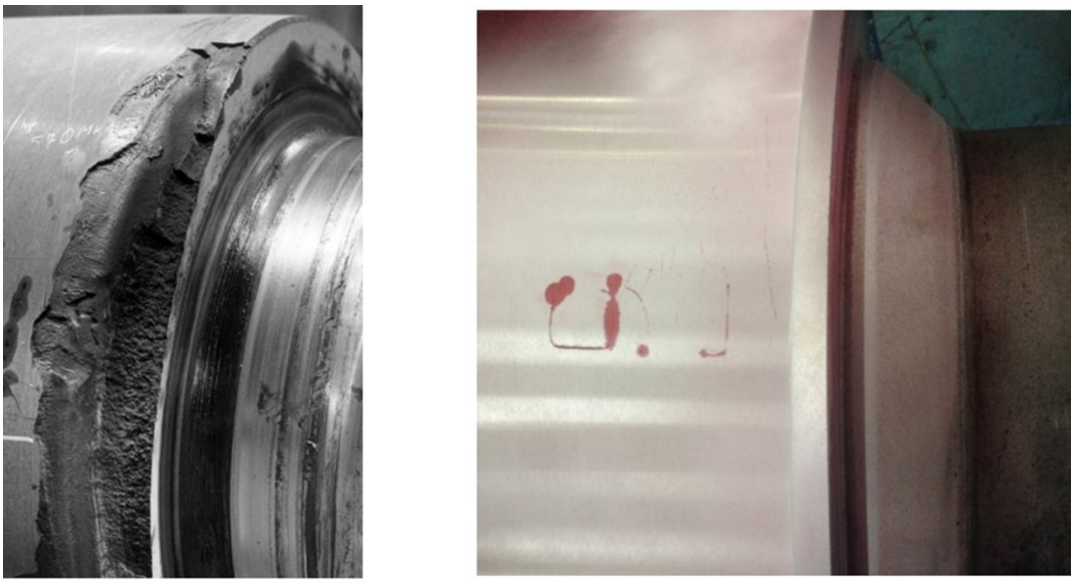

(a) (b)

Figure 1. Roll failures produced for stress concentration: (**a**) Backup Roll spalling; (**b**) Work Roll cracks.

It is impossible to avoid elastic deformation of the rolls due to the rolling loads, and this could be critical, in combination with stress concentration and crown shape. There is always a latent risk of an operational accident, yet such risk can be reduced with a more complete understanding of the rolling process. Useful predictive data can be collected by FEM of rolls as a double cantilever model with the fulcrum of beams in a centerline mill.

According to previous studies, CVC is the best geometry for pressure distribution control in BURs [4,5]. However, this geometry requires grinding machines with controls and many mills do not have access to them. Thus, it is essential to carry out this study considering traditional positive, negative and flat-shaped crowns. In addition, the fact that the thermal crown resembles a positive crown, and the wear on the rolls of a negative crown must be taken into account.

2. Materials and Methods

The deformation of the rolls is directly related to the dimensions of the rolls, the support points and the application of rolling loads, as shown in the schematic of Figure 2.

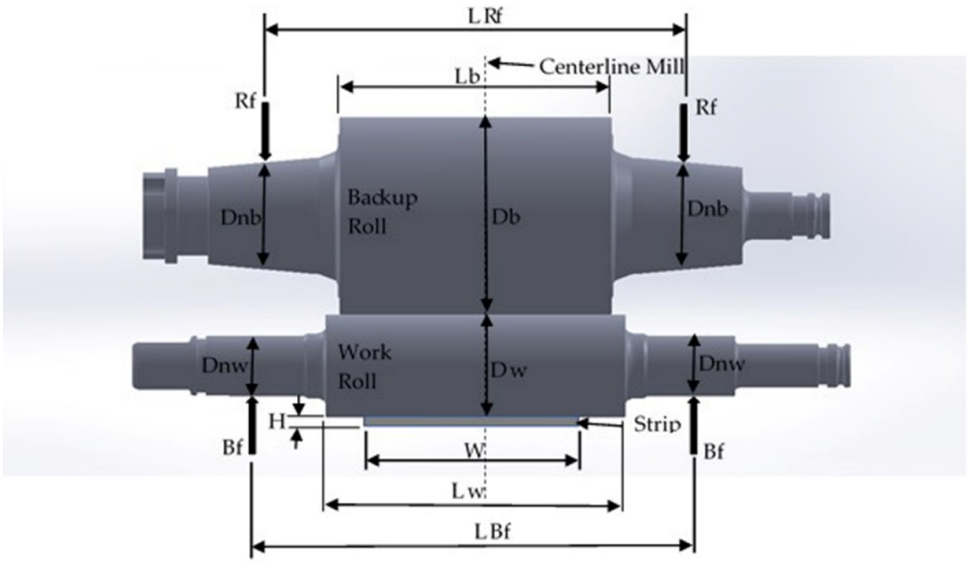

Figure 2. Schematic of the main dimensional variables for four high rolling mill.

The forces causing the work roll deformation include rolling force, inter-roll force, and work roll bending force. Work roll deflection at element i is described by Jiang et al. and Wang [20,21] and can be expressed as:

$$y_W(i) = \sum_{j=1}^{n} g_W(i,j)(q(j) - p(j)) - g_{FW}(i)F_W, \tag{1}$$

where y_W (i) is the vertical deformation of the work roll at element i, g_W (i, j) is the work roll deflection influence function due to the combined bending and shear forces generated by rolling and inter-roll force at element j; pi is the rolling force at element i. qj is the contact force between work roll and backup roll at element j. F_W is the work roll bending force, g_{FW} (i) is the work roll bending influence function due to the work roll bending force.

The backup roll deflection is caused only by the inter-roll force, so backup roll deflection at element i can be expressed as [20,21]:

$$y_B(i) = \sum_{j=1}^{n} g_B(i,j)q(j), \tag{2}$$

where y_B (i) is the vertical deformation of the backup roll at element i, g_B (i, j) is the backup roll deflection influence function due to the combined bending and shear forces generated by inter-roll force at element j.

The force causing flattening between the work roll and the strip is the rolling force, and the force causing the flattening between the work roll and backup roll is the inter-roll force. Therefore, the flattening at element i can be expressed as [20,21]:

$$y_{WS}(i) = \sum_{j=n_L}^{n_R} g_{WS}(i,j)p(j) \tag{3}$$

$$y_{WB}(i) = \sum_{j=1}^{2n} g_{WB}(i,j)p(j), \tag{4}$$

where g_{WS} (i, j) is the flattening influence function of work roll and strip due to the rolling force at element j; n_L and n_R are the element numbers at the left and right edges of the strip according to the second numbering rule; g_{WB} (i, j) is the flattening influence function of the work roll and the backup roll due to the inter-roll force at element j.

The analyses of the distribution of stress and the deformation of rolls for the rolling process are based on an FEM employing ANSYS Mechanical Static Structural, considering the main variables and conditions in the process of rolling and described by the parameters in Table 1. The rolling and bending forces are uniformly distributed, and are applied in the bearing areas. The rolls and strip are considered to behave flexibly, with general joints in the lateral face, which only allow for vertical movement in the direction of force application and roll deformation. The mesh for all the simulations had 461,800 nodes and 240,076 elements, with two zones of hexahedral elements with 20 nodes and tetrahedral elements with 10 nodes. The contact region mesh is refined using 20 layers with a growth rate of 1.1. Moreover, there are two contact zones, one of them between BUR and WR and the other one between WR and Strip. To avoid slipping of components in the contact zones, a bonded system is implemented without penetration.

Table 1. Parameter of the three dimensions finite element model of roll stacks.

Model Parameter	Value
Work roll diameter Dw	650.875 mm
Work roll barrel length Lw	1897.20 mm
Work roll neck diameter Dnw	384.175 mm
Work roll Bending force length LBf	2747.20 mm
Backup roll diameter Db	1244.60 mm
Backup roll barrel length Lb	1727.20 mm
Backup roll neck diameter Dnb	678.49 mm
Backup roll Rolling force length LRf	2717.80 mm
Strip width W	1574.8 mm
Strip thickness H	2.5 mm
Rolling force Rf	38,000 kN
Bending force Bf	400 kN
Poisson's ratio work roll	0.3
Poisson's ratio backup roll	0.3
Young's modulus work roll	210 GPa
Young's modulus backup roll	220 GPa
Work Roll Crown	0.1016 mm
Backup Roll Crown	0.0762 mm
Young's modulus strip	210 MPa
Maximum Thermal crown WR	0.150 mm
Maximum Thermal crown BUR	0.100 mm
Maximum wear WR	0.200 mm
Maximum wear BUR	0.525 mm

The data considered for the analysis are those established for stand M-5 of a hot rolling mill, in which the materials of the rolls are 5% Cr-forged steel for the backup roll and nodular iron Indefinite Chilled Double Pour (ICDP) for the work roll, rolling a structural steel.

According to previous studies by Wang et al. and Cao et al. [4,5], the best pressure distribution is obtained by CVC crown; therefore, it is considered the worst case, and analysis of such combinations are used for positive, negative and flat crowns. When considering a thermal crown, the heat generated in the roll expands the material forming a positive crown according to Chang, Galantucci and Tricarico, Hacquin et al. and Zhao et al. [7–10]. Thus, we considered a thermal crown of 0.100 mm for the backup rolls and 0.150 mm for the work rolls.

According to the calculations made by Liu et al. and Rumualdo et al. [6,15], it has been established that the greatest wear occurs in the center of the rolls based on the wear parameters. According to the

periods of the rolling campaigns, these are much longer for the backup rolls, with at least fourteen days of continuous operation. The values considered critical are 0.200 mm and 0.525 mm for the work and backup rolls, respectively, and negative crowns with these values will be used to simulate wear. Finally, the use of flat geometries is applied to get an idea of the behavior when crowns are not used, or when the thermal crown compensates for the wear generated.

The analysis of the distribution of stress and deformation of rolls for the rolling process is based on a FEM considering all the possible combinations of crown shape (positive, negative, and flat), as shown in Table 2.

Table 2. Combinations of crown shape analyzed.

Combination	Configuration
1	BUR Positive–WR Positive
2	BUR Positive–WR Flat
3	BUR Positive–WR Negative
4	BUR Flat–WR Positive
5	BUR Flat–WR Flat
6	BUR Flat–WR Negative
7	BUR Negative–WR Positive
8	BUR Negative–WR Flat
9	BUR Negative–WR Negative

3. Results

The distribution of stress and the total deflection along the barrel length were obtained for the work and backup rolls from simulation results of the rolling process with the parameters shown in Table 1. The simulations considered the most important configuration, the different types of crown shape on roll barrel (three levels: Positive, Flat and Negative) and a strip with a constant width of 1574.8 mm.

3.1. Characteristics of Rolling Stress along Barrel Length of Work and Backup Rolls

Figure 3a–c show the results of stress distribution for a backup roll with positive crown, combining the mechanical contact with a work roll using a positive, flat and negative crown, respectively.

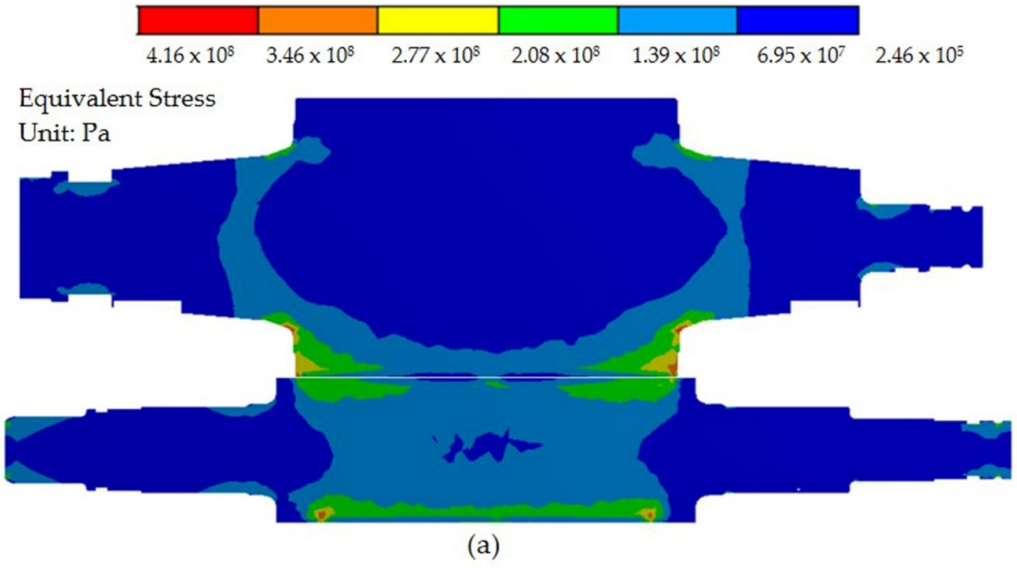

Figure 3. *Cont.*

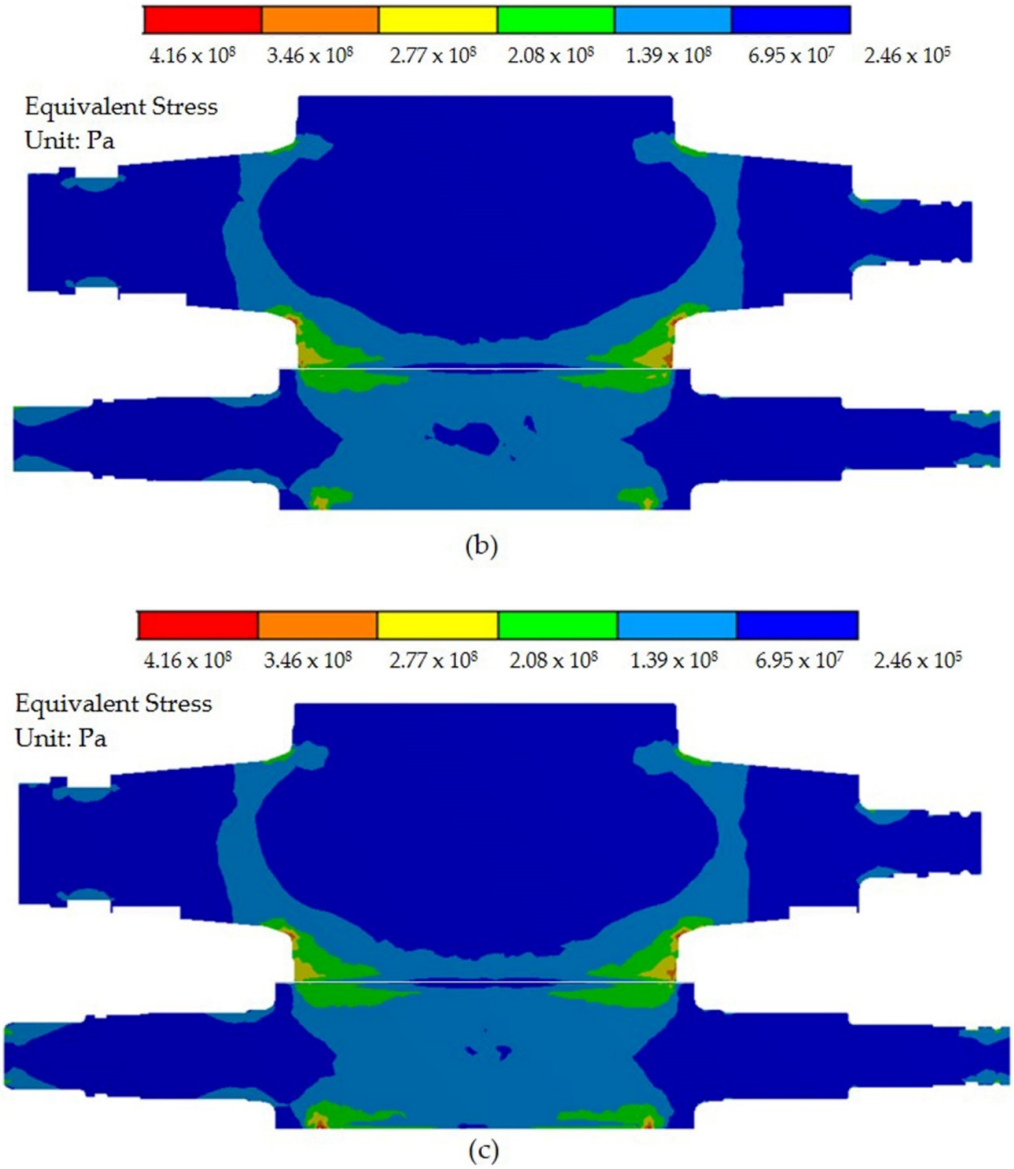

Figure 3. Stress distribution for combinations of crowns: (**a**) combination 1, (**b**) combination 2, and (**c**) combination 3.

In all three cases shown in Figure 3, stress concentration is observed at both ends at 787.4 mm from the center of the mill, coincident with the sides of the strip. For work rolls, the area that is in direct contact with the strip is the most critical, reaching values of 200 MPa for combination 1 (Figure 3a) and 3 (Figure 3c); and for the backup rolls stress concentration is observed at the same point at 787.4 mm and in the main radius due to the change of section, the maximum stress is very similar due to the appearance of the figures. However, for combination 3 (Figure 3c), the stress is slightly less, at 252.0 MPa. In this case, the best option for work rolls is combination 2 (Figure 3b), at 171.0 MPa, and for backup rolls, combination 3 (Figure 3c) is the best option, at 252.0 MPa.

Figure 4a–c show the results of stress distribution for a backup roll without a crown (flat), combining the mechanical contact with a work roll that uses positive crown, flat and negative crown, respectively.

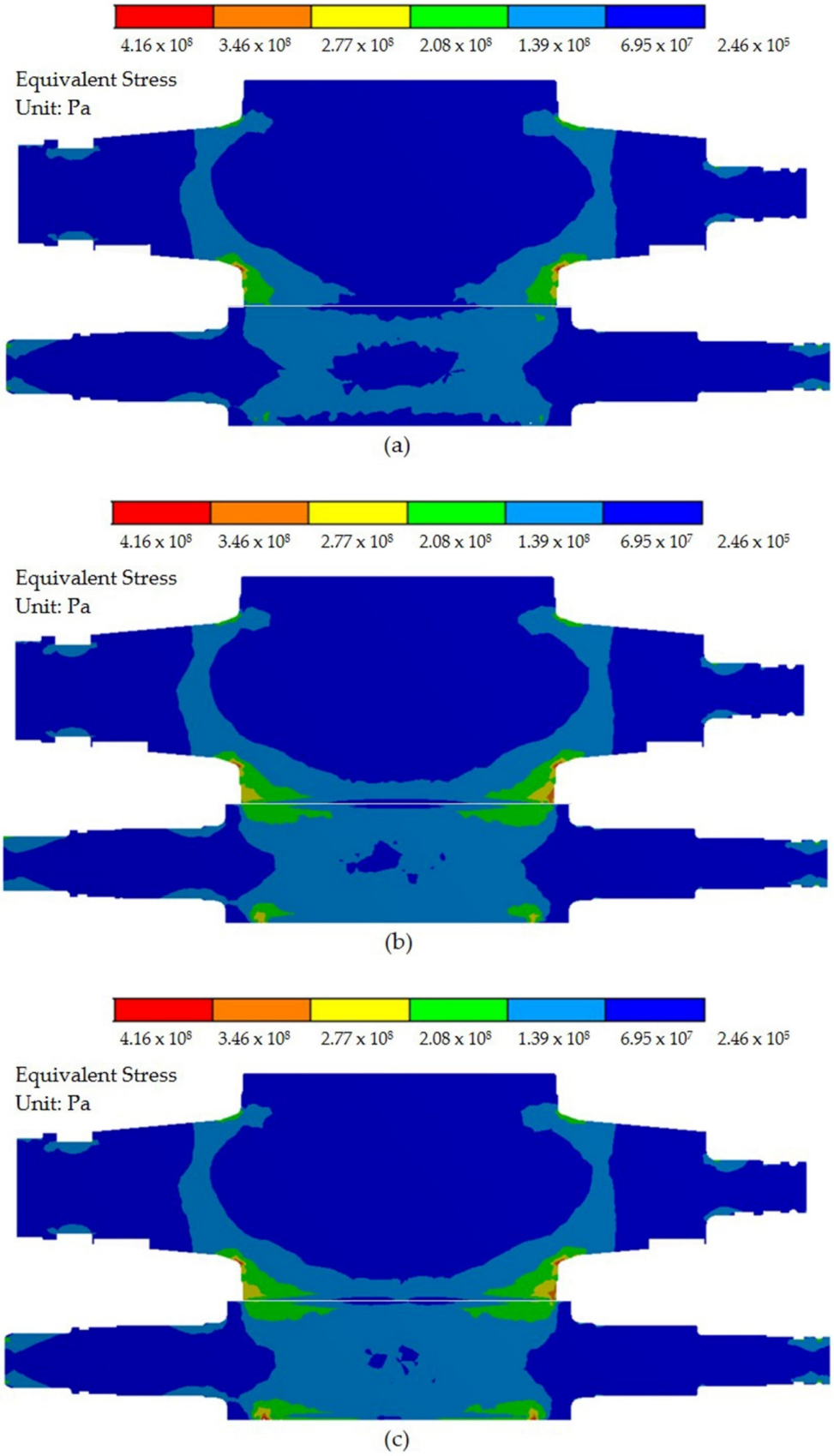

Figure 4. Stress distribution for combinations of crown: (**a**) combination 4, (**b**) combination 5, and (**c**) combination 6.

The behavior of these three combinations in Figure 4 shows a phenomenon very similar to the one described above. Yet, in these three combinations the values are slightly lower, and for combination 4 (Figure 4a) the maximum stress for the BUR is only manifested in the main radius, and not in the contact area with the work roll, and its maximum value is 163.0 MPa. In the case of the work roll, the minimum stress found is for combination 4 (Figure 4a), which has 121.0 MPa. For combinations 5 (Figure 4b) and 6 (Figure 4c), stress concentration is observed at both ends 787.4 mm from the center of the mill, on the sides of the strip. In this case, the best option for work and backup rolls is combination 4 (Figure 4a).

Figure 5a–c show the results of stress distribution for negative crown BUR, combining the mechanical contact with a WR using positive crown, flat, and negative crown, respectively.

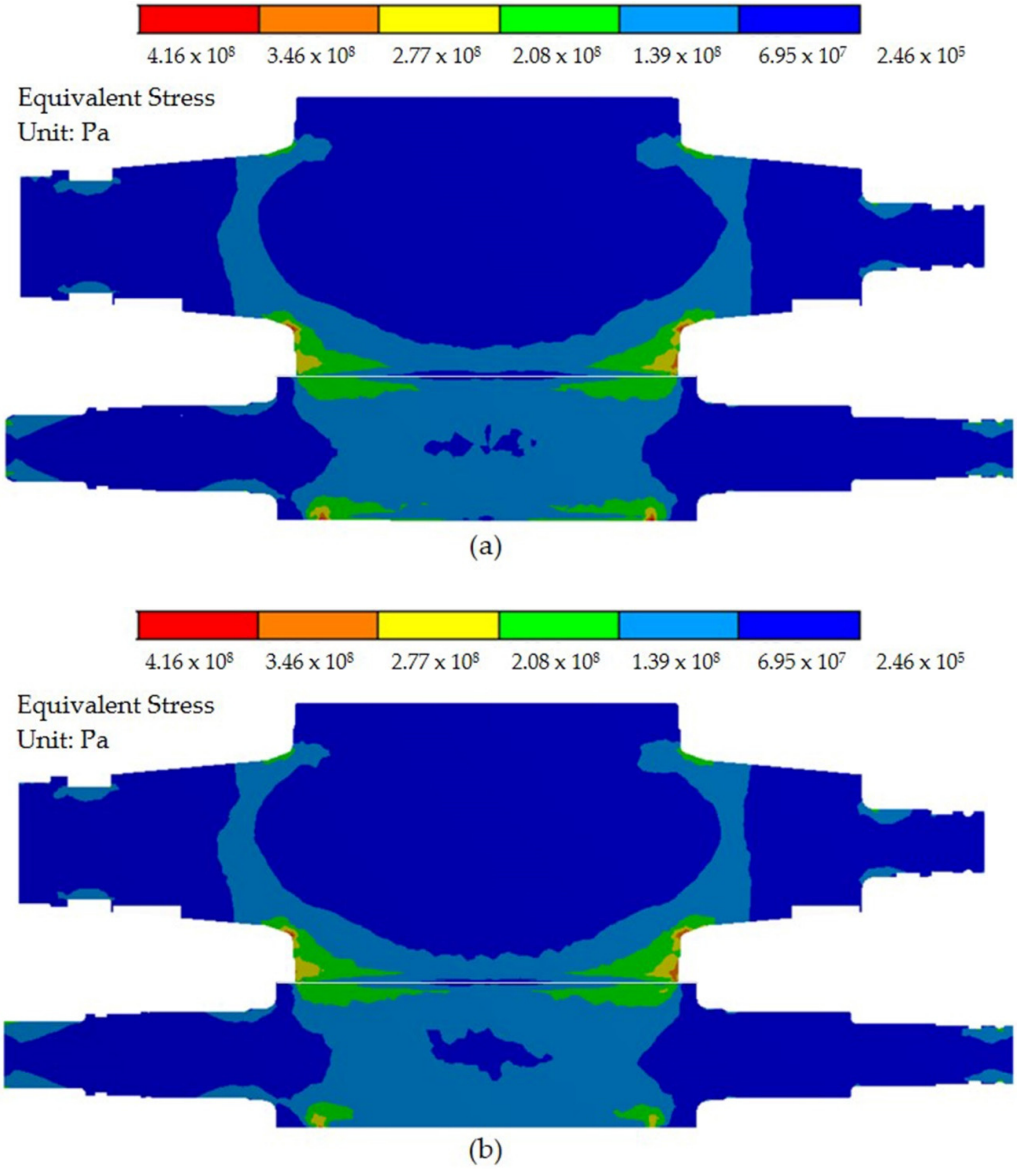

Figure 5. *Cont*.

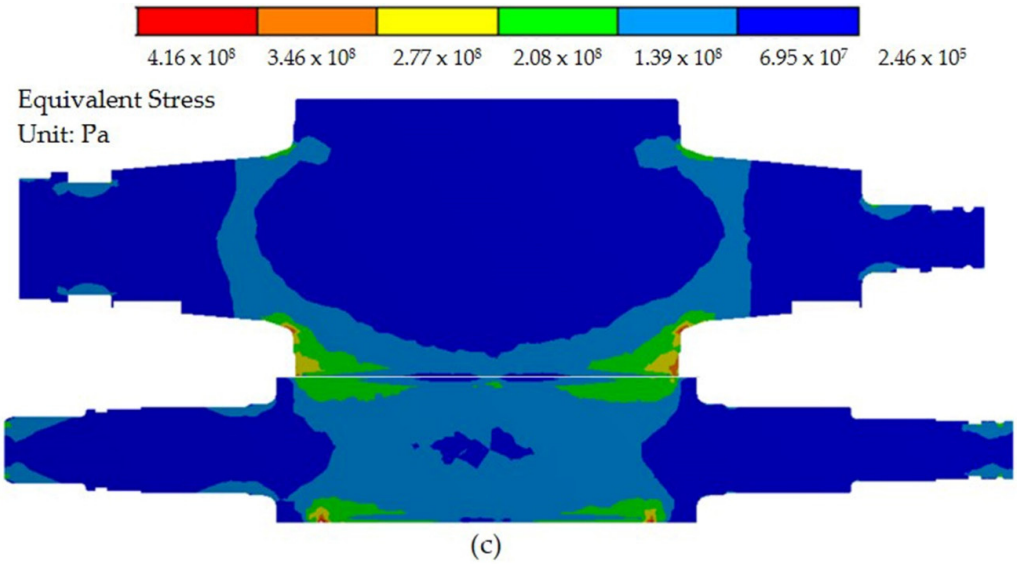

Figure 5. Stress distribution for combinations of crown: (**a**) combination 7, (**b**) combination 8 and (**c**) combination 9.

In all three cases in Figure 5, stress concentration is observed at both ends at 787.4 mm from the center of the mill, on the slides of the strip. For WRs, the area that is in direct contact with the strip is the most critical, reaching values of 203.0 MPa for combinations 7 (Figure 5a) and 9 (Figure 5c), and for the BUR, stress concentration is observed at the same point at 787.4 mm and in the main radius due to the change of section. Also, the maximum stress is very similar, as can be observed in the figures. However, for combination 8 (Figure 5b) the stress is slightly less, at 196.0 MPa. In this case, the best option for work and backup rolls is combination 8 (Figure 5b).

In the nine combinations analyzed, it can be observed that for both work and backup rolls, the maximum stress value is concentrated at 787.4 mm from the center of the mill, which matches exactly with the edges of the strip; and particularly for the WR, the critical area is the one in direct contact with the strip generating a maximum stress of 258.0 MPa. For BURs, in addition to the maximum stress generated by the contact of the rolls, a concentration point of stress is produced in the main radius with the same magnitude of the maximum stress (271.0 MPa). The mechanical contact due to stress is more critical on BURs, because concentration points are generally observed at the end of the barrel and in the main radius of the neck. This supports the notion that when the yield limits are exceeded, the BUR suffers spalling while the WR only presents surface cracks.

As for the combinations of crowns, it can be observed that the worst results are obtained when the geometries are the same for work and backup rolls, for example combinations 1 (BUR Positive–WR Positive), 5 (BUR Flat–WR Flat) and 9 (BUR Negative–WR Negative).

3.2. *Characteristics of Roll Deflection along the Barrel Length of Work and Backup Rolls*

Figure 6a–c show the results of roll deflection distribution for a positive crown backup roll, combining the mechanical contact with a work roll using positive crown, flat, and negative crown, respectively.

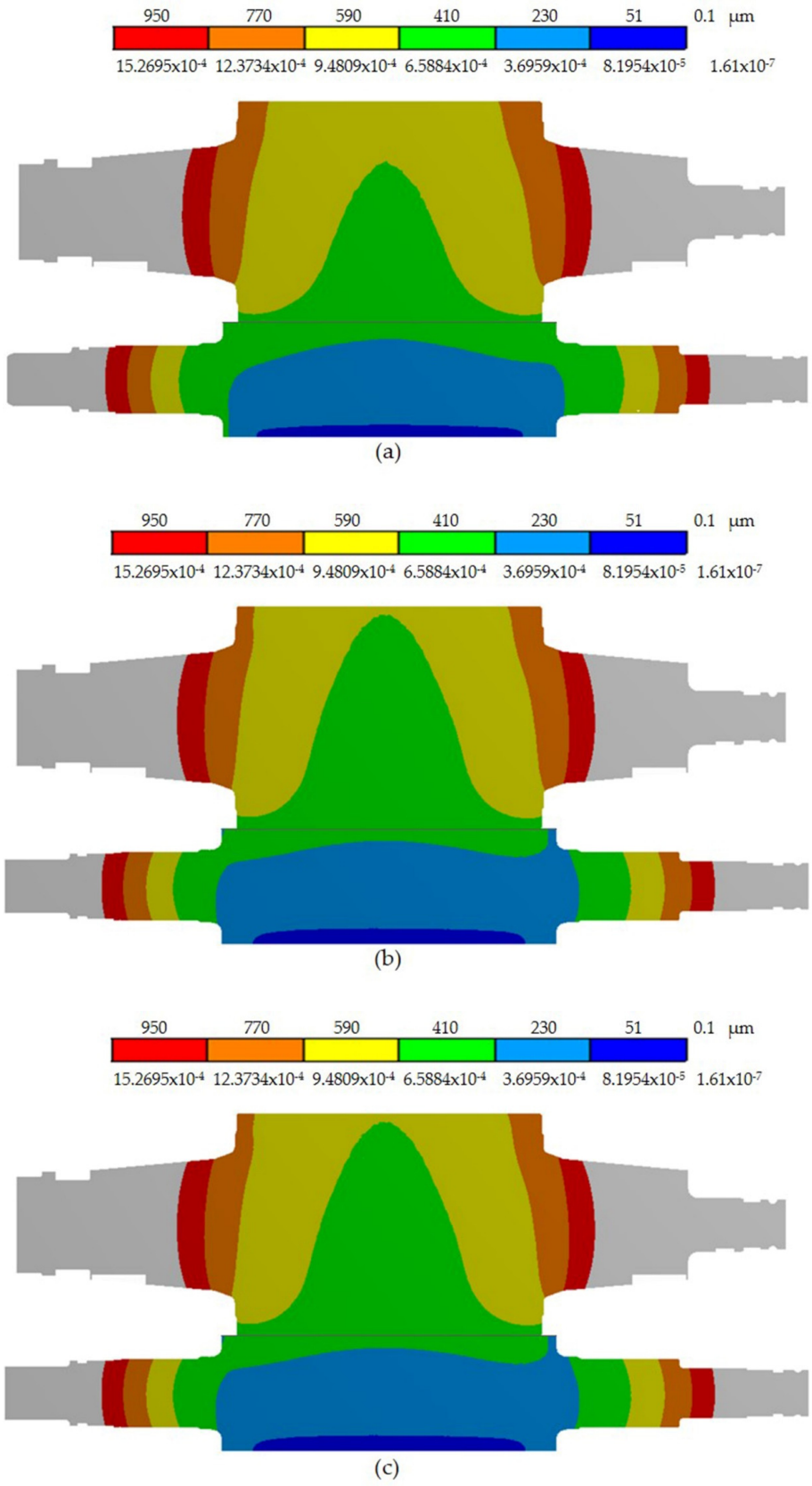

Figure 6. Roll deflection distribution for combinations of crown: (**a**) combination 1, (**b**) combination 2, and (**c**) combination 3.

For all three cases in Figure 6, the same performance behavior is observed, where the work roll has minimal deflection because on one side it is in contact with the strip and on the other end it is in contact with the BUR. This generated deflection is minimal and irrelevant for its analysis. However, the deflection of the BUR is considerable and always maintains the same pattern, with minor deflection observed in the area of contact with the WR and maximum deflection being distributed towards the barrel length ends. For the three cases analyzed, the largest strain is obtained with combination 1 (Figure 6a), reaching values of 400 µm, which is equivalent to 6.4276×10^{-4}.

Figure 7a–c show the results of roll deflection distribution for a BUR without a crown (Flat), combining the mechanical contact with a WR that uses positive crown, flat, and negative crown, respectively.

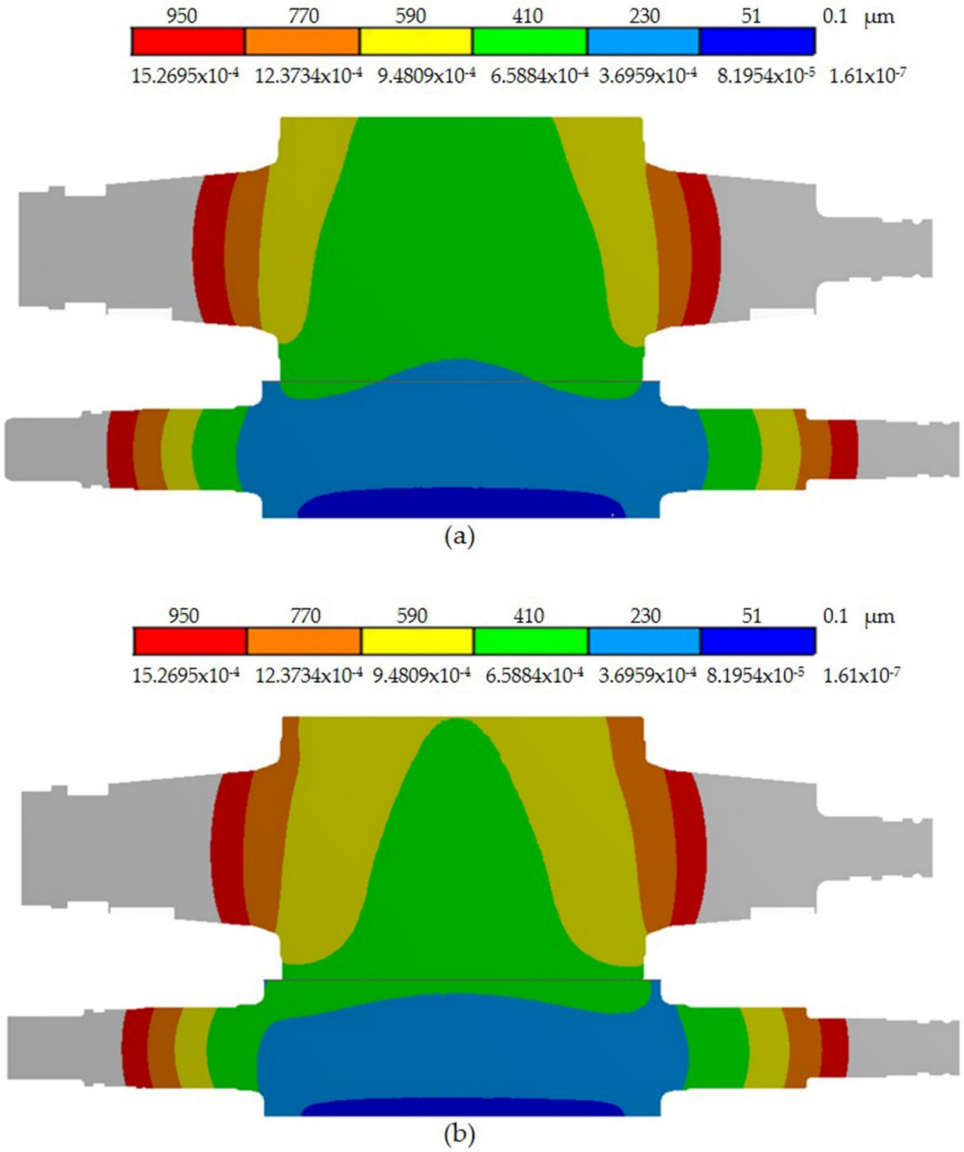

Figure 7. *Cont.*

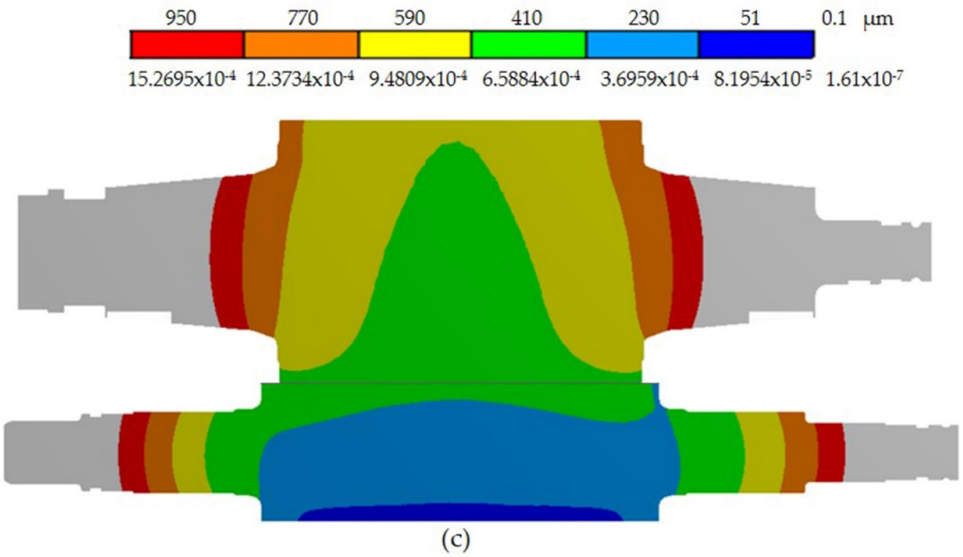

Figure 7. Roll deflection distribution for combinations of crown: (**a**) combination 4, (**b**) combination 5, and (**c**) combination 6.

For all three cases in Figure 7, the pattern in the work and backup rolls is the same as that described above for Figure 6. Only the deflection values for the backup rolls change slightly: minor deflection is observed in the contact area with the WR and maximum deflection towards the ends of the barrel length. For the three cases analyzed, the lowest deflection was obtained with combination 4 (Figure 7a), obtaining strain only at the ends of the barrel length, with a value of 4.8369×10^{-4}, which is equivalent to 301 µm.

Figure 8a–c, show the results of roll deflection distribution for a BUR with a negative crown, combining the mechanical contact with WR using positive crown, flat, and negative crown, respectively.

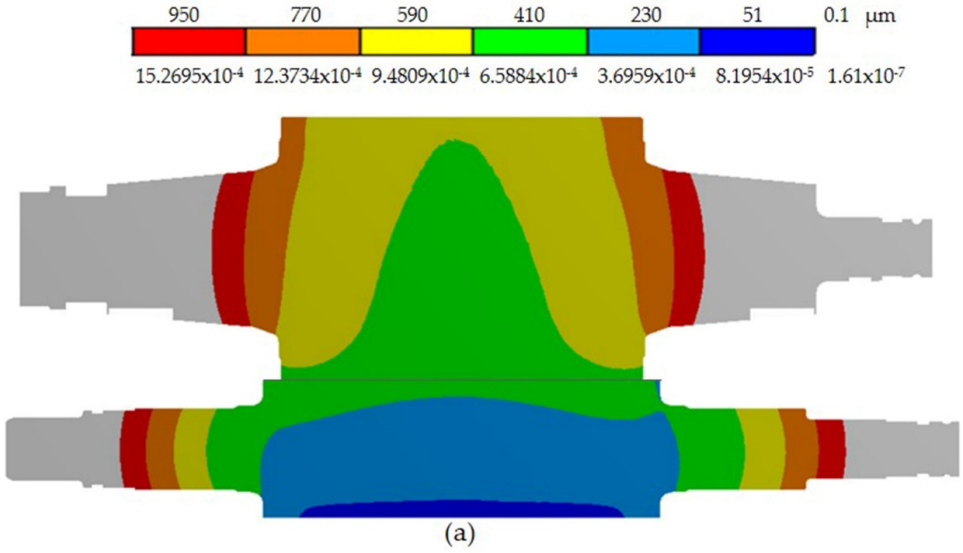

Figure 8. *Cont.*

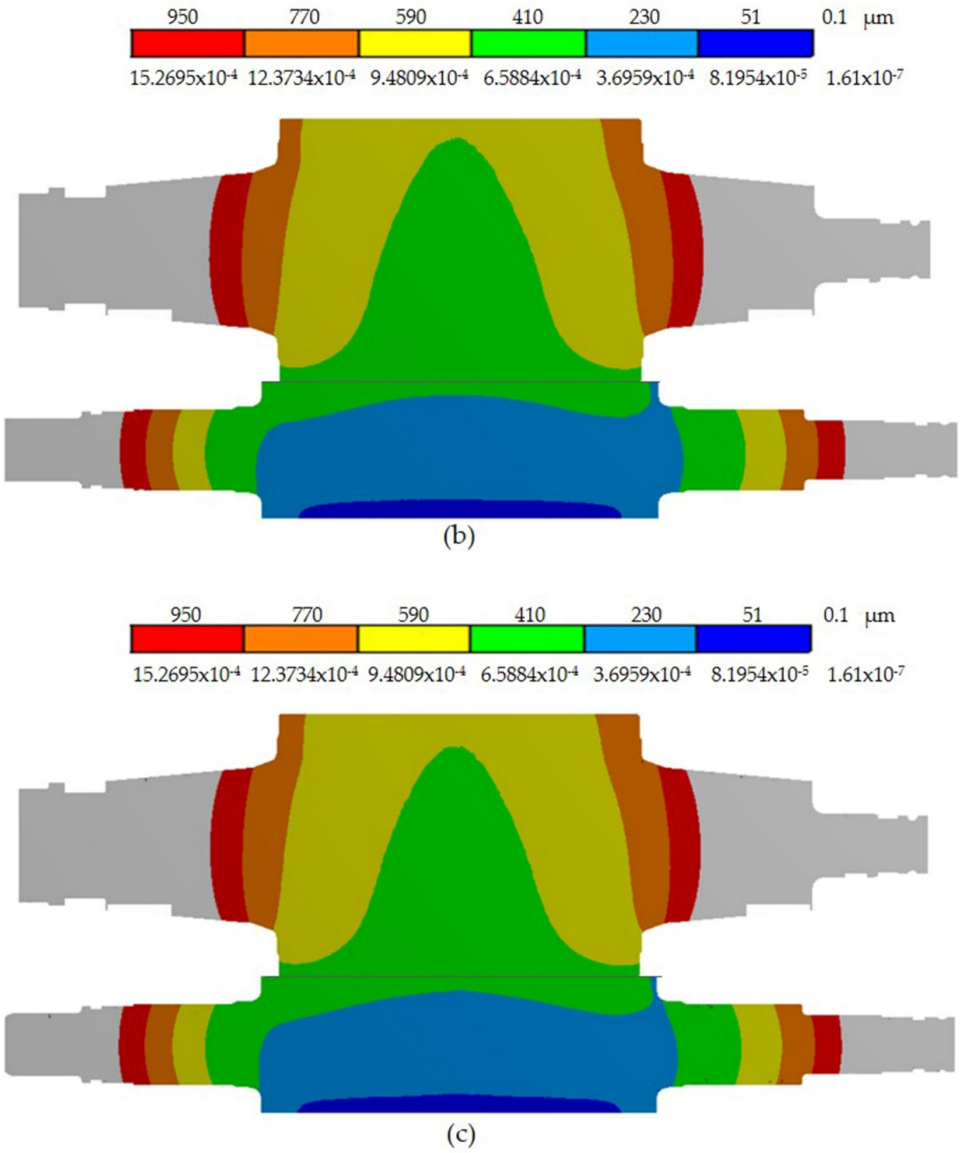

Figure 8. Roll deflection distribution for combinations of crown: (**a**) combination 7, (**b**) combination 8, and (**c**) combination 9.

For all three cases in Figure 8, the pattern in the work and backup rolls is exactly the same as that described above for Figures 6 and 7. It is only possible to appreciate that the surface with strain of 6.1867×10^{-4} (equivalent to 385 µm) at the ends of the barrel length occupies more area for combination 9 (Figure 8c) than for combinations 7 (Figure 8a) and 8 (Figure 8b).

In the nine combinations analyzed (Figures 6–8), it can be observed that the deflection for the WR is negligible because the mechanical contact with the strip and the BUR prevents deflection.

For all the combinations of Figures 6–8, roll deflection on BURs is symmetrical; however, for WR in Figure 6b,c, Figure 7b,c and Figure 8a–c, there is an unsymmetrical behavior of roll deflection due to the contact model used for the coupling of the drive side.

4. Discussion

From the results presented in Figures 3–5, it can be concluded that for all cases, the rolling forces also cause a point of concentration of stress in the main radius of the union between the Barrel Length and the Neck, which has the same magnitude of the maximum stress generated at the end of the Barrel Length.

In Figure 9, all the stress values generated for all nine analyzed combinations are plotted. It can be concluded that the pattern of the graph is the same for the backup rolls, with the stress being concentrated at both ends at 787.4 mm from the center of the mill, on the sides of the strip. The best result of the options analyzed is for combination 4 (BUR Flat–WR Positive), with a maximum stress of 163.0 MPa, and the worst case is for combination 1 (BUR Positive–WR Positive), with 271.0 MPa. It can also be concluded that the highest stress concentration values are obtained when the geometries of the bodies of both rollers are the same. This takes place in combinations 1 (BUR Positive–WR Positive), 5 (BUR Flat–WR Flat) and 9 (BUR Negative–WR Negative).

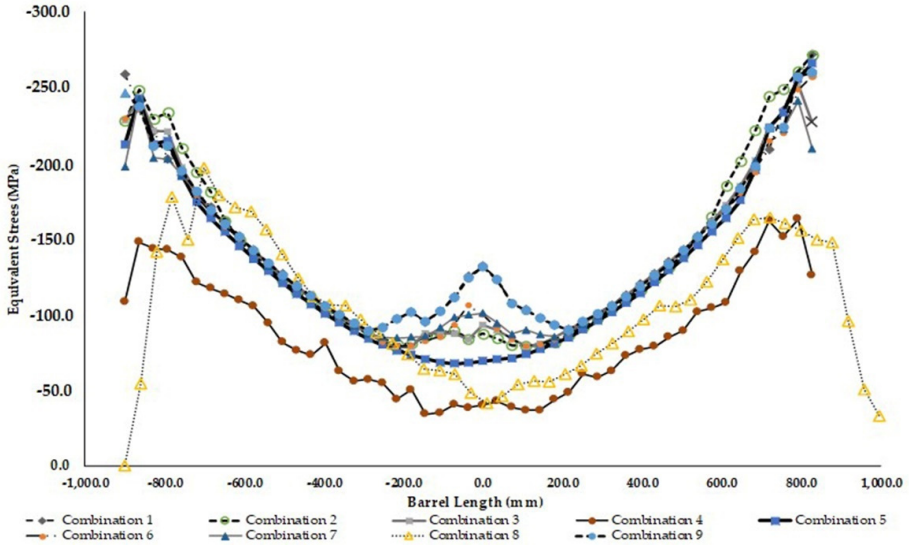

Figure 9. Graph of the stress distribution curves for all mechanical contact combinations analyzed on BUR.

For the particular case presented in this study, analyzing the possible behavior of the stress distribution on the BUR for a rolling campaign, the expected results would be those shown in Figure 10. The best combination of shape would be to start with combination 4 (BUR Flat–WR Positive) yielding a maximum stress of 163.0 MPa, and at the end of the campaign change the crown of the work roll to flat, thus adopting combination 8 (BUR Negative–WR Flat, BUR Negative due to wear) yielding a maximum stress of 196.0 MPa, as shown in the graph in Figure 10.

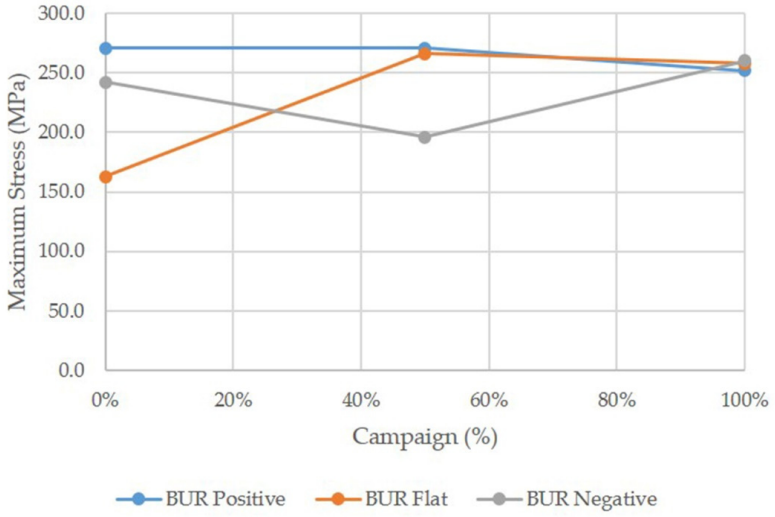

Figure 10. Expected stress distribution behavior for different combinations of contact geometries during a rolling campaign of a BUR.

In Figure 11, all the values of the deformations generated for the nine combinations analyzed are plotted. It can be concluded that the pattern of the graph is the same for the backup rolls, with the maximum deformation being concentrated at both ends at 787.4 mm from the center of the mill, on the sides of the strip. The best results (with less deformation) are for combination 4 (BUR Flat–WR Positive), with a maximum strain of 4.8368×10^{-4} (301 µm), and the worst case scenario is for combination 1 (BUR Positive–WR Positive), with a maximum strain of 6.4277×10^{-4} (400 µm). It can also be concluded that the largest values of deformation are obtained when the geometries of the bodies of both rolls are the same, that is, in combinations 1 (BUR Positive–WR Positive), 5 (BUR Flat–WR Flat), and 9 (BUR Negative–WR Negative).

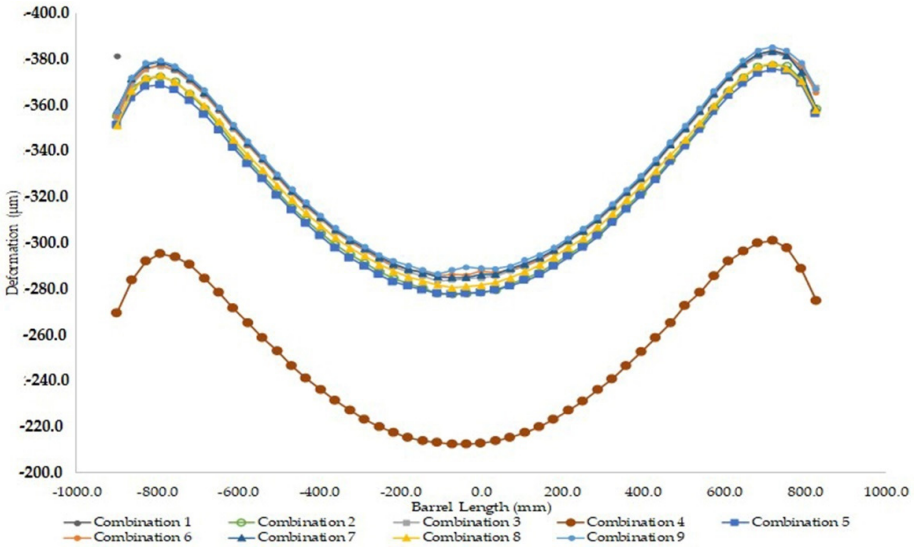

Figure 11. Graph of deformation distribution curves for all mechanical contact combinations analyzed.

The profiles of the graphs in Figures 9 and 11 are very similar, indicating a similar behavior of deformation and stress, confirming the relationship between stress and strain established by the first Hooke's law.

5. Conclusions

According to the results, for industrial conditions in this specific analysis, it is recommended to use combination 4 (BUR Flat–WR positive) at the beginning of the rolling campaign. In addition, at the end of the campaign of BURs, changes to flat WR crowns are suggested. Under these conditions, the combinations of crown shape will help on the effect of pressure distribution on BURs.

Author Contributions: R.S. Conceived and designed the simulations, S.A.A. and I.C. performed the simulations and wrote the paper, A.P. and S.M.S.M. analyzed the data.

Funding: This research received no external funding.

Acknowledgments: This work was supported by the Universidad Autónoma de Coahuila.

Conflicts of Interest: The authors declare no conflict of interest.

References

1. Guanghui, Y.; Jianguo, C.; Jie, Z.; Shenghui, J.; Renwei, T. Backup roll contour of a Smart Crown tandem cold rolling mil. *J. Univ. Sci. Technol. Mater.* **2008**, *15*, 357–361.
2. Li, H.; Xu, J.; Wang, G.; Shi, L.; Xiao, Y. Development of Strip Flatness and Crown Control Model for Hot Strip Mills. *J. Iron Steel Res. Int.* **2010**, *17*, 21–27. [CrossRef]

3. Wang, X.D.; Li, F.; Li, B.H.; Zhu, G.S.; Li, B.; Zhang, B.H. VCR back-up roll and negative work roll contour design for solving roll spalling and transfer bar profile problems in hot strip mil. *Ironmak. Steelmak.* **2010**, *37*, 633–640. [CrossRef]
4. Wang, X.D.; Li, F.; Li, B.H.; Zhu, G.S.; Li, B. Design and Application of an Optimum Backup Roll Contour Configured with CVC Work Roll in Hot Strip Mill. *ISIJ Int.* **2012**, *52*, 1637–1643. [CrossRef]
5. Cao, J.; Wei, G.; Zhang, J.; Chen, X.; Zhou, Y. VCR and ASR technology for profile and flatness control in hot strip mills. *J. Cent. South. Univ. Technol.* **2008**, *15*, 264–270. [CrossRef]
6. Liu, G.; Li, Y.; Huang, Q.; Yang, X. Axial Force Analysis and Roll Contour Configuration of Four-High CVC Mill. *Math. Probl. Eng.* **2018**, *2018*. [CrossRef]
7. Der-Form, C. Thermal stresses in work rolls during the rolling of metal strip. *J. Mater. Process. Technol.* **1999**, *94*, 45–51. [CrossRef]
8. Galantucci, L.M.; Tricarico, L. Thermo-mechanical simulation of a rolling process with an FEM approach. *J. Mater. Process. Technol.* **1999**, *92–93*, 494–501. [CrossRef]
9. Hacquin, A.; Montmitonnet, P.; Guillerault, J.-P. A steady state thermo-elastoviscoplastic finite element model of rolling with coupled thermo-elastic roll deformation. *J. Mater. Process. Technol.* **1996**, *60*, 109–116. [CrossRef]
10. Zhao, N.; Cao, J.; Zhang, J.; Su, Y.; Yan, T.; Rao, K. Work roll thermal contour prediction model of nonoriented electrical steel sheets in hot strip mills. *J. Univ. Sci. Technol. Beijing Mater.* **2008**, *15*, 352–356. [CrossRef]
11. Li, Y.; Cao, J.; Yang, G.; Dun, W.; Zhou, Y.; Ma, H. ASR Bending Force Mathematical Model for the Same Width Strip Rolling Campaigns in Hot Rolling. *Steel Res. Int.* **2014**, *86*, 567–575. [CrossRef]
12. Spuzic, S.; Strafford, K.N. Wear of hot rolling mill rolls: An overview. *Wear* **1994**, *176*, 261–271. [CrossRef]
13. Turk, R.; Fajfar, P.; Robic, R.; Perus, I. Prediction of hot strip mill roll wear. *Metalugija* **2002**, *41*, 47–51.
14. Li, C.S.; Liu, X.H.; Wang, G.D.; Yang, G. Experimental investigation on thermal wear of high speed steel rolls in hot strip Rolling. *Mater. Sci. Technol.* **2002**, *18*, 1581–1584. [CrossRef]
15. Rumualdo Servin, A.; Garcia, R.M. Development of Mathematical Model for Control Wear in Backup Roll for Hot Strip Mill. *J. Iron Steel Res. Int.* **2014**, *21*, 46–51. [CrossRef]
16. Liu, X.; Xu, S.; Li, S.; Xu, J.; Wang, G. FEM Analysis of Rolling Pressure Along Strip Width in Cold Rolling Process. *J. Iron Steel Res. Int.* **2007**, *14*, 22–26. [CrossRef]
17. Zhang, G.; Xiao, H.; Wang, C. Three-Dimensional Model for Strip Hot Rolling. *J. Iron Steel Res. Int.* **2006**, *13*, 23–26. [CrossRef]
18. Kong, N.; Cao, J.; Wang, Y.; Tieu, A.; Kiet, Y.; Hou, L.; Wang, Z. Development of Smart Contact Backup Rolls in Ultrawide Stainless Strip Rolling Process. *Mater. Manuf. Process.* **2014**, *29*, 129–133. [CrossRef]
19. Cao, J.; Chai, X.; Li, Y.; Kong, N.; Jia, S.; Zeng, W. Integrated design of roll contours for strip edge drop and crown control in tandem cold rolling mills. *J. Mater. Process. Technol.* **2018**, *252*, 432–439. [CrossRef]
20. Jiang, Z.Y.; Wei, D.; Tieu, A.K. Analysis of cold rolling of ultra thin strip. *J. Mater. Process. Technol.* **2009**, *209*, 4584–4589. [CrossRef]
21. Wang, G.D. *The Shape Control and Theory*; Metallurgical Industry Press: Beijing, China, 1986; pp. 246–249.